

Development of an AAV-CRISPR-Cas9-based treatment for dominant cone-rod dystrophy 6

Russell W. Mellen,¹ Kaitlyn R. Calabro,¹ K. Tyler McCullough,¹ Sean M. Crosson,¹ Alejandro de la Cova,¹ Diego Fajardo,¹ Emily Xu,¹ Sanford L. Boye,² and Shannon E. Boye¹

¹Division of Cellular and Molecular Therapy, Department of Pediatrics, University of Florida, Gainesville, FL, USA; ²Powell Gene Therapy Center, Department of Pediatrics, University of Florida, Gainesville, FL, USA

Cone-rod dystrophy 6 (CORD6) is caused by gain-of-function mutations in the *GUCY2D* gene, which encodes retinal guanylate cyclase-1 (RetGC1). There are currently no treatments available for this autosomal dominant disease, which is characterized by severe, early-onset visual impairment. The purpose of our study was to develop an adeno-associated virus (AAV)-CRISPR-Cas9-based approach referred to as “ablate and replace” and evaluate its therapeutic potential in mouse models of CORD6. This two-vector system delivers (1) CRISPR-Cas9 targeted to the early coding sequence of the wild-type and mutant *GUCY2D* alleles and (2) a CRISPR-Cas9-resistant cDNA copy of *GUCY2D* (“hardened” *GUCY2D*). Together, these vectors knock out (“ablate”) expression of endogenous RetGC1 in photoreceptors and supplement (“replace”) a healthy copy of exogenous *GUCY2D*. First, we confirmed that ablation of mutant R838S *GUCY2D* was therapeutic in a transgenic mouse model of CORD6. Next, we established a proof of concept for “ablate and replace” and optimized vector doses in *Gucy2e*^{+/-}:*Gucy2f*^{-/-} and *Gucy2f*^{-/-} mice, respectively. Finally, we confirmed that the “ablate and replace” approach stably preserved retinal structure and function in a novel knockin mouse model of CORD6, the RetGC1 (hR838S, hWT) mouse. Taken together, our results support further development of the “ablate and replace” approach for treatment of CORD6.

INTRODUCTION

Gain-of-function mutations in retinal guanylate cyclase 2D (*GUCY2D*) are the leading cause of dominant cone-rod dystrophies, accounting for 35% of cases.¹ Patients with *GUCY2D*-associated cone-rod dystrophy 6 (CORD6) experience early-onset cone cell loss with variable rod involvement, which leads to loss of central/color vision, nystagmus, photophobia, and degeneration of the macula beginning in the first decade of life. By the third decade, the majority of CORD6 patients have no remaining cone-mediated vision.² Most CORD6-causing mutations are localized to a nucleotide mismatch at or near residue 838 of the encoded protein.^{3,4} The variations in disease onset/progression reflect the heterogeneity in the underlying mutations, with one of the most severe disease presentations caused by a transversion resulting in arginine-838 substitution by serine (R838S).⁵

GUCY2D encodes retinal guanylate cyclase 1 (RetGC1), a protein expressed in photoreceptor outer segments.⁶ Light stimulation causes hydrolysis of cyclic guanosine monophosphate (cGMP) by cGMP phosphodiesterase 6 (PDE6).⁷ The reduction of available cGMP leads to closure of cGMP-gated ion channels, which causes a reduction of intracellular Ca²⁺ and hyperpolarization of photoreceptors.^{8,9} When intracellular Ca²⁺ levels are high, Ca²⁺-bound guanylate cyclase-activating proteins (GCAPs) inhibit RetGC1 activity.¹⁰ When intracellular Ca²⁺ levels drop, Mg²⁺-bound GCAPs activate RetGC1.¹⁰ This interplay ensures that RetGC1 is only active when photoreceptors are hyperpolarized by light.¹¹ CORD6-associated mutations cause conformational changes in RetGC1 that favor binding of Mg²⁺-bound GCAPs, altering calcium sensitivity and leaving the enzyme in a constitutively active state.¹² The dysregulation of RetGC1 in the outer segments causes photoreceptor dysfunction but accounts for only a portion of the CORD6 phenotype. Retinal degeneration 3 (RD3) protein is expressed exclusively in the inner segments of photoreceptors and strongly represses RetGC1 function in that compartment by displacing GCAP from the cyclase during trafficking to the outer segments.^{13,14} Constitutive GCAP-mediated activation of RetGC1 in the outer segment,¹⁵ together with its aberrant activation in the inner segment, leads to rapid-onset photoreceptor cell death.^{16,17} RD3 binds heterodimers of R838S mutant/wild-type (WT) RetGC1 with lower affinity than either form of RetGC1 homodimer (WT:WT or mutant:mutant).¹⁸ Additionally, the heterodimer binds Mg²⁺-bound GCAP with much higher affinity than either form of homodimer.¹⁸ For this reason, it is hypothesized that photoreceptor dysfunction in CORD6 patients relates to constitutive activation of RetGC1 in the outer segments, aggravated by aberrant activation of RetGC1 heterodimers in the inner segments.

Traditional gene replacement is not sufficient to treat CORD6 because the gain-of-function allele must be removed. We previously established a proof of concept that an adeno-associated virus (AAV)-CRISPR-Cas9 system could efficiently disrupt the WT *Gucy2e*

Received 7 February 2023; accepted 30 May 2023;
<https://doi.org/10.1016/j.omtm.2023.05.020>

Correspondence: Shannon E. Boye, Division of Cellular and Molecular Therapy, Department of Pediatrics, University of Florida, PO Box 100296, Gainesville, FL 32610, USA.

E-mail: shaire@ufl.edu



and *GUCY2D* loci in mice and macaques, respectively, knocking out RetGC1 expression in the injected retinas of both species.¹⁹ This indiscriminatory, mutation-agnostic approach, which targets the same early coding sequence in each allele, is attractive because of the heterogeneous etiology of *CORD6* (it avoids development and verification of a new CRISPR-Cas9 system for each individual mutation). Building on this result, here we propose use of an “ablate and replace” approach to address *CORD6*, whereby AAV is used to co-deliver (1) CRISPR-Cas9 to disrupt both *GUCY2D* alleles (WT and mutant) and (2) a Cas9-resistant (“hardened”) copy of *GUCY2D* to provide normal RetGC1 function. We first evaluated reagents in R838S transgenic (R838S Tg) mice, which harbor random insertions of *CORD6*-causing human *GUCY2D*-R838S.^{11,20} R838S Tg mice model the retinal degeneration seen *CORD6* patients but not their genetic landscape (chromosomal location/copy numbers and photoreceptor cell type expression pattern). To address this discrepancy, we developed a novel knockin mouse model that accurately recapitulates the *CORD6* genotype, the RetGC1 (hR838S, hWT) mouse. Similar to patients, this mouse model exhibits progressive loss of retinal structure and function. Finally, we provide evidence in RetGC1 (hR838S, hWT) mice that an AAV-CRISPR-Cas9-based “ablate and replace” approach is therapeutic in a genetic landscape similar to the human *CORD6* condition and lay the groundwork for clinical application of this approach.

RESULTS

AAV-CRISPR-Cas9-based gene editing preserves retinal structure and function in a Tg mouse model of *CORD6*

R838S Tg mice harbor random insertions of R838S *GUCY2D* cDNA under control of the rhodopsin promoter. They exhibit early-onset, progressive rod degeneration; aberrant rod morphology; and no evidence of a cone cell phenotype (because of rod-specific expression of the mutant transgene mediated by the rhodopsin promoter).^{11,20} While R838S Tg mice are an imperfect model of *CORD6* because of the random insertions of a mutant transgene into the genome, expression in rods only (versus rods and cones), and residual expression of endogenous WT *Gucy2e*, they do have a phenotype (retinal degeneration) against which we could score the effects of gene editing. Our strategy took advantage of the species specificity of our guide RNA (gRNA) to edit/knock out the deleterious R838S *GUCY2D* allele while leaving the endogenous *Gucy2e* allele intact. Because of the early-onset degeneration seen in these mice, subretinal injections were carried out at first eye opening (~post-natal day 15). Right (OD) eyes were injected with AAV-*SaCas9* and AAV-*GUCY2D* gRNA-*GFP* at a 1:1 ratio. Contralateral eyes served as a no-editing control and were injected with AAV-*GUCY2D* gRNA-*GFP* alone. Mice were treated with a low [3E9 vector genomes (vg)/eye] or high (3E10 vg/eye) dose (Table 1).

AAV-CRISPR-Cas9 treatment significantly preserved photoreceptor structure relative to that seen in control eyes. This was observed as early as 4 and 8 weeks post injection (p.i.) at the low and high dose, respectively (Figures 1A and 1B). Outer nuclear layer (ONL) preservation in treated eyes was stable over 32 weeks p.i., the latest time

point evaluated. At 36 weeks p.i., retinal sections from mice in the low-dose cohort were immunostained for rhodopsin to label the rod outer segments and counterstained with DAPI. Transduced cells were identified by AAV-mediated GFP expression. In addition to markedly reduced ONL thickness, photoreceptors in retinas treated with control vector exhibited shortened inner segments (ISs) and outer segments (OSs). In contrast, retinas treated with editing reagents exhibited thicker ONLs and longer, properly organized OSs, confirming that editing of the mutant R838S *GUCY2D* sequence in R838S Tg mice preserved photoreceptor nuclei and IS/OS length (Figure 1C). Despite this maintenance of retinal structure, neither treatment dose resulted in significant improvement in rod-mediated function at any time point tested (Figure S1). At 36 weeks p.i., animals were sacrificed, and eyes were collected for analysis. Neural retinas treated with doses of 3E9 vg/eye (n = 7) and 3E10 vg/eye (n = 4) underwent UDiTaS analysis to quantify on-target editing rates achieved at each dose.²¹ Editing rates of 8.45% and 20.1% were observed in the low- and high-dose cohorts, respectively. Because (1) subretinally injected AAV vectors do not transduce all retinal cells, (2) the hGRK1 promoter restricts expression of editing reagents to photoreceptors, and (3) only a fraction of the neural retina is comprised of photoreceptors, these values significantly underrepresent the overall editing efficiency in the target cell.

Significant and stable preservation of photoreceptors and rod morphology in R838S Tg mice provides support for a gene editing-based approach to treat *CORD6*. However, R838S Tg mice are a problematic model for further progressing our “ablate and replace” approach because they endogenously express RetGC1 and RetGC2 via *Gucy2e* and *Gucy2f*, respectively, and therefore do not allow evaluation of the “replace” arm of this approach.

Establishing a proof of concept for “ablate and replace”

We previously demonstrated the ability to “replace” by delivering therapeutic *Gucy2e* to photoreceptors via AAV to treat models of recessive *GUCY2D*-associated Leber congenital amaurosis.^{22,23} We have also demonstrated the ability to “ablate” by knocking out *Gucy2e* and *GUCY2D* using AAV-CRISPR-Cas9 in mice and macaques, respectively.¹⁹ The “ablate and replace” system combines these two approaches by knocking out the mutant and WT alleles of *Gucy2e*/*GUCY2D* with AAV-CRISPR-Cas9, and supplementing them with a CRISPR-Cas9-resistant (“hardened”) copy of *Gucy2e*/*GUCY2D* in *trans* (Figure 2A). A similar system has been used to successfully treat a mouse model of autosomal dominant retinitis pigmentosa.^{24,25} Our murine CRISPR-Cas9 system targets exon 2 of *Gucy2e*, well upstream of the exon harboring the *CORD6* mutation site in the homologous *GUCY2D* gene.¹⁹ *In silico* analysis confirmed that our gRNA is unlikely to induce off-target editing in the murine genome.¹⁹ The “hardened” *Gucy2e* cDNA contains five silent mutations in the gRNA recognition site and two silent mutations in the protospacer adjacent motif (PAM) sequence (Figure 2B). Because of the limited packaging capacity of AAV, elements of the “ablate and replace” system had to be divided between two vectors, with the first vector containing the gRNA upstream of the “hardened” *Gucy2e* and the second containing

Table 1. A summary of all *in vivo* experiments performed

Mouse line	OD injection	OS injection	Doses	
Gene editing in R838S Tg mice				
R838S Tg	AAV.SPR-hGRK1-SaCas9 + AAV.SPR-U6- <i>GUCY2D</i> gRNA-hGRK1-GFP	AAV.SPR-U6- <i>GUCY2D</i> gRNA-hGRK1-GFP	3E9 vg/eye 3E10 vg/eye	
Mouse line	Group	OD injection	OS injection	Dose
A + R in <i>Gucy2e</i> ^{+/-} : <i>Gucy2f</i> ^{-/-} mice				
<i>Gucy2e</i> ^{+/-} : <i>Gucy2f</i> ^{-/-}	treatment	AAV.SPR- hGRK1-SaCas9 + AAV.SPR-U6- <i>Gucy2e</i> gRNA-hGRK1-‘hardened’ <i>Gucy2e</i>	AAV.SPR-hGRK1-SaCas9 + AAV.SPR-U6- <i>Gucy2e</i> gRNA-hGRK1-GFP	3E9 vg/eye
	RetGC1 “toxicity control”	AAV.SPR-U6- <i>Gucy2e</i> gRNA-GRK1-‘hardened’ <i>Gucy2e</i>	vehicle	3E9 vg/eye
Mouse line	Group	OD injection	OS injection	Doses
“Ablate only” dose-ranging study in <i>Gucy2f</i> ^{-/-} mice				
<i>Gucy2f</i> ^{-/-}	treatment	AAV.SPR-hGRK1-SaCas9 + AAV.SPR-U6- <i>Gucy2e</i> gRNA-hGRK1-Dead-RetGC1	vehicle	1E8 vg/eye 3E8 vg/eye 1E9 vg/eye 3E9 vg/eye
	Cas9 “toxicity control”	AAV.SPR-hGRK1-SaCas9 + AAV.SPR-U6-control gRNA-hGRK1-Dead-RetGC1	vehicle	1E8 vg/eye 3E8 vg/eye 1E9 vg/eye 3E9 vg/eye
Mouse line	OD injection	OS injection	Doses	
“Replace only” dose-ranging study in <i>Gucy2e</i> ^{-/-} mice				
<i>Gucy2e</i> ^{-/-}	AAV.SPR-U6- <i>Gucy2e</i> gRNA-hGRK1-“hardened” <i>Gucy2e</i>	vehicle	1E8 vg/eye 3E8 vg/eye 1E9 vg/eye 3E9 vg/eye	
Mouse line	OD injection	OS injection	Dose	
A+ R in RetGC1 (hR838S, hWT) mice				
RetGC1 (hR838S, hWT)	AAV.SPR- hGRK1-SaCas9 + AAV.SPR-U6- <i>Gucy2e</i> gRNA-hGRK1-“hardened” <i>Gucy2e</i>	vehicle	1E9 vg/eye	
RetGC1 (hWT, hWT)	vehicle	vehicle	N/A	

SaCas9 (Table 1). The system was designed so that the combined Cas9 and gRNA expression will occur only when the same cell is transduced by both vectors, ensuring that editing could not occur in the absence of exogenous, “hardened” *Gucy2e*.

The “ablate and replace” system was first tested in *Gucy2e*^{+/-}:*Gucy2f*^{-/-} mice (Figure 2A). This model was chosen because it relies on a single *Gucy2e* allele to support retinal guanylate cyclase activity. *Gucy2e*^{+/-}:*Gucy2f*^{-/-} mice lack a retinal phenotype, but it was anticipated that knocking out the remaining copy of *Gucy2e* (via editing) would lead to robust retinal degeneration as seen in RetGC1/RetGC2 double knockout (*Gucy2e*^{-/-}:*Gucy2f*^{-/-}, here referred to as GCdko) mice.^{19,26,27} We compared the efficacy of the “ablate and replace” system to an “ablate only” system. Right eyes were subretinally injected with the “ablate and replace” vectors (AAV-*Gucy2e* gRNA-“hardened” *Gucy2e* + AAV-*SaCas9*), and left eyes were subretinally injected with the “ablate” vectors alone (AAV-*Gucy2e* gRNA-GFP + AAV-*SaCas9*). An additional cohort of mice received subretinal injections of the

AAV-*Gucy2e* gRNA-“hardened” *Gucy2e* vector in their right eyes to control for any potential negative impacts of overexpressing “hardened” *Gucy2e*. Their left eyes were injected with vehicle (buffered saline solution [BSS]) to control for the impact of subretinal surgery itself (Table 1). Each vector was injected at a dose of 3E9 vg/eye, with eyes receiving two vectors having a total viral load of 6E9 vg/eye.

At 20 weeks p.i., significant preservation of scotopic (rod-mediated) and photopic (cone-mediated) function (Figures 2C and 2D) and significant preservation of ONL thickness (Figure 2E) were observed in the eyes of *Gucy2e*^{+/-}:*Gucy2f*^{-/-} mice that received “ablate and replace” vectors relative to “ablate only” controls. However, rod- and cone-mediated function and ONL thickness in the “ablate and replace” eyes remained significantly reduced relative to vehicle-injected controls. Eyes from the “hardened only” control group also showed significantly reduced scotopic and photopic electroretinography (ERG) responses and ONL thickness relative to vehicle-injected controls. These results provided a proof of concept for use of the

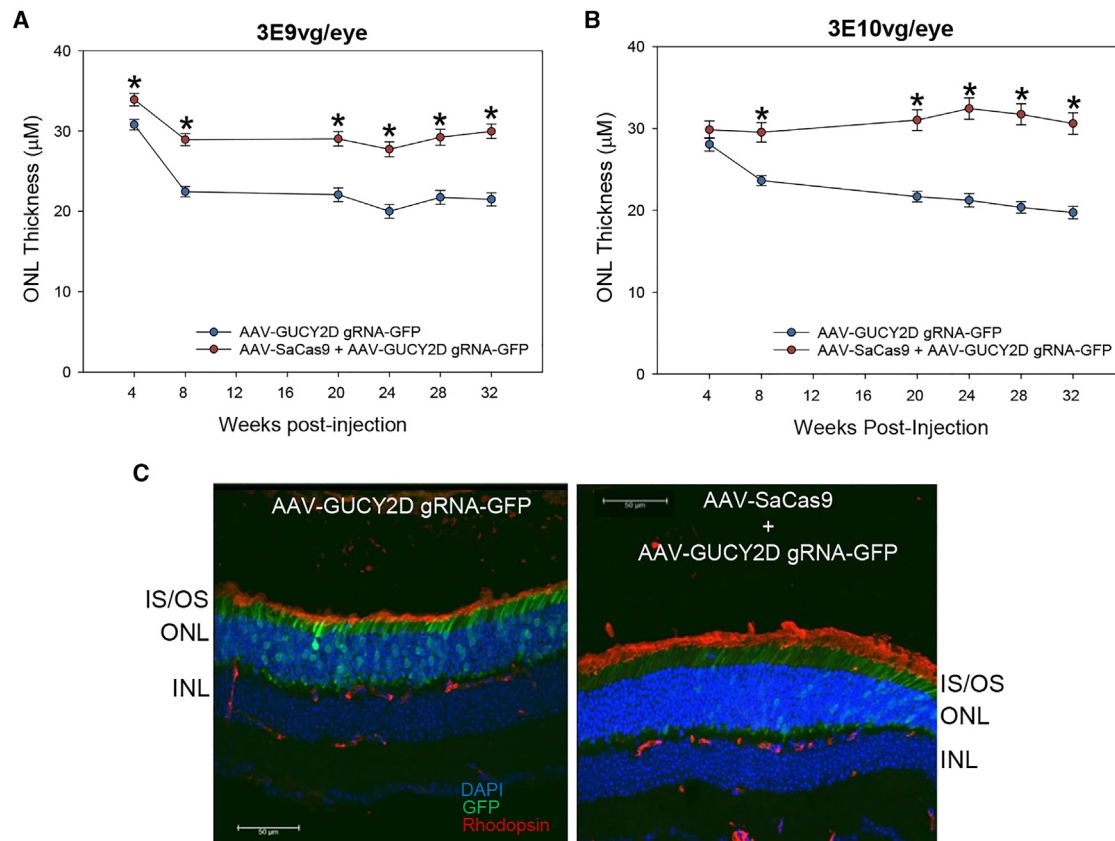


Figure 1. AAV-CRISPR-Cas9 preserves retinal structure in the R838S Tg mouse model of CORD6

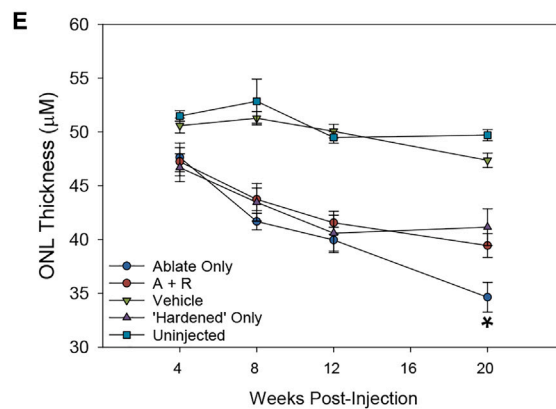
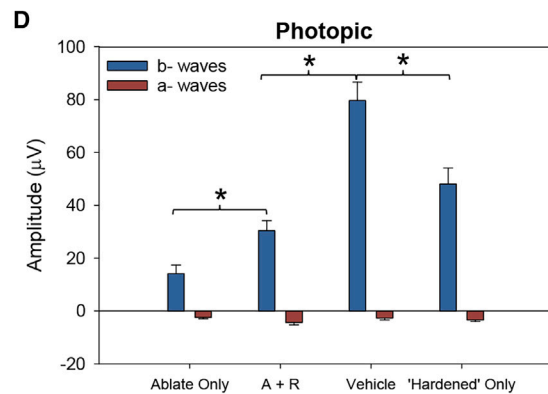
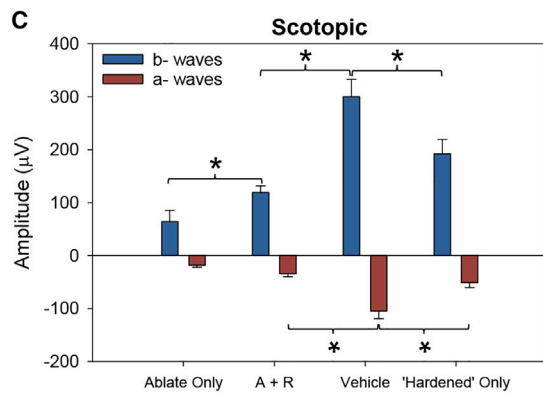
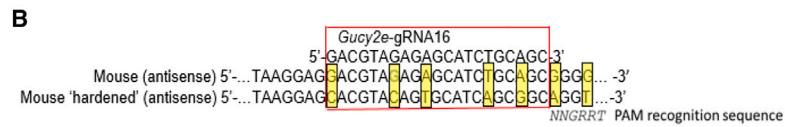
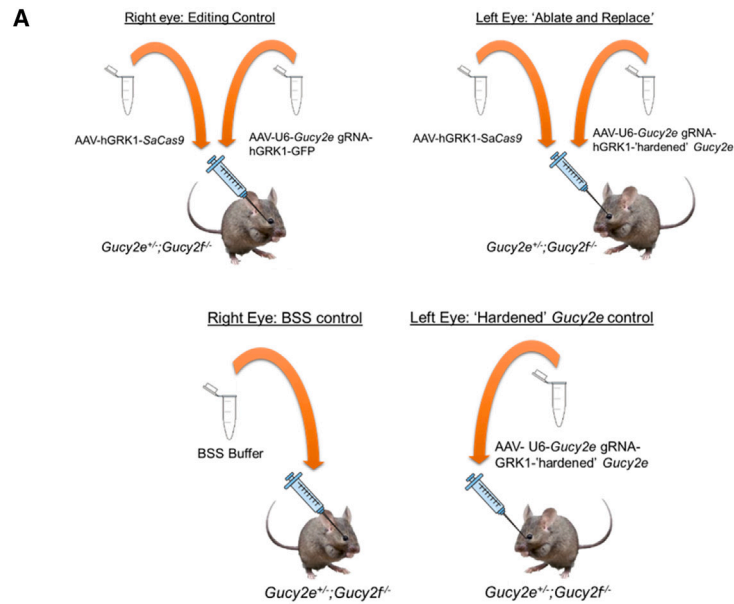
(A and B) The outer nuclear layer (ONL) is significantly thicker and stably maintained in eyes treated at a dose of 3E9 vg/eye (A) and 3E10 vg/eye (B). A two-way ANOVA followed by a post-hoc Tukey's range test was performed ($p < 0.05$). (C) Representative images of retinal cross-sections from R838S Tg mice taken at 36 weeks p.i. with either control vector (AAV-GUCY2D gRNA-GFP, left) or AAV-SaCas9 and AAV-GUCY2D gRNA-GFP (right) at a dose of 3E9 vg/eye. All images were taken at 40 \times magnification. Retinas were immunostained for rhodopsin (red) and counterstained with DAPI (blue). GFP (green) shows raw expression (no immunostain). Scale bars in (C), 50 μ m.

“ablate and replace” system in a mouse model otherwise lacking an underlying retinal phenotype. However, the significant reductions in retinal structure/function in eyes injected with only “hardened” *Gucy2e* vector at 3E9 vg/eye confirmed and the fact that eyes injected with “ablate and replace” reagents had reduced retinal structure/function relative to vehicle controls suggested that further dose optimization was warranted.

Optimizing doses of the “ablate and replace” CRISPR-Cas9 vectors

Dose-ranging studies were performed to optimize the doses of the requisite “ablate and replace” components. The first study sought to determine the minimum dose of editing reagents required to induce a physiological response. For this purpose, we cloned a stop codon into the “hardened” *Gucy2e* gene directly downstream of the would-be gRNA recognition site to create a truncated RetGC1 (“deadGC1”) lacking the entire cytoplasmic portion (Figure 3A). This ensured that only the editing elements (CRISPR-Cas9) of the

system were active. *Gucy2f*^{-/-} mice have no associated phenotype because of the presence of *Gucy2e*. Editing of both *Gucy2e* alleles in this model, however, would induce a RetGC-null state and lead to profound retinal degeneration, as described previously.^{27,28} This model was chosen to assess editing capability because editing of two *Gucy2e* alleles is required to observe a physiological effect, and the ability to edit two alleles will ultimately be essential for treating CORD6 via this approach. Right eyes of *Gucy2f*^{-/-} mice were injected with AAV-SaCas9 and AAV-Gucy2e-deadGC1 in equal proportion. Left eyes were injected with vehicle alone. Cohorts of mice ($n = 4-7$) were subretinally injected with each vector at a dose of 1E8 vg/eye, 3E8 vg/eye, 1E9 vg/eye, or 3E9 vg/eye (Table 1). Retinal degeneration was used as an indirect measure of biallelic, on-target editing (editing of a single allele is insufficient to cause retinal degeneration).¹⁹ At 24 weeks p.i., there was a dose-dependent decline in scotopic and photopic ERG responses (Figures 3B and 3C). Statistically significant reductions in scotopic and photopic b-wave amplitudes were observed at doses of 3E8 vg/eye and above. Injection of



(legend on next page)

AAV-*SaCas9* and AAV-*Gucy2e*-deadGC1 at the two highest doses (1E9 vg/eye and 3E9 vg/eye) also led to significant ONL thinning starting at 8 weeks p.i. that progressed through the end of the study (Figure 3D). By 24 weeks p.i., the 1E9 vg/eye treatment group had a 20% reduction in ONL thickness, while the dose of 3E9 vg/eye had a 37% reduction compared with vehicle controls (Figure 3E). There were no detectable changes in ONL thickness in eyes injected with 1E8 vg/eye or 3E8 vg/eye at any time point. Subretinal injections of our editing reagents at 3E8 vg/eye led to a significant decline in photoreceptor function but did not cause structural degeneration. Doses of 1E9 vg/eye and 3E9 vg/eye led to significant declines in photoreceptor function and number. Therefore, 1E9 vg/eye was selected as the minimum dose of editing reagents required to produce a biologically meaningful level of editing in injected animals.

Using retinal degeneration as a measure of on-target editing is potentially problematic because we cannot distinguish between degeneration caused by on-target *Gucy2e* editing vs. that caused by potential toxic overexpression of Cas9. For this reason, we took advantage of the species specificity of our gRNAs and subretinally injected additional cohorts of *Gucy2f*^{-/-} mice (n = 5) with AAV-*SaCas9* and AAV-*GUCY2D* gRNA-deadGC1 (primate-specific guide). Contralateral eyes were injected with vehicle alone. Together, these vectors express a stable CRISPR-Cas9 system that is incapable of editing murine *Gucy2e*, meaning any observed retinal degeneration will have been caused by toxic overexpression of Cas9. Vectors delivered at a dose of 1E9 vg/eye did not lead to any significant changes in photoreceptor function or structure for at least 24 weeks p.i. compared with vehicle controls (Figures S2A and S2B). The dose of 3E9 vg/eye caused significant loss of photoreceptor structure, but not function, at 24 weeks p.i. (Figures S2C and S2D). These results suggested that AAV-mediated Cas9 delivered at a dose of 3E9 vg/eye is detrimental to retinal health over the long term. These results contrast what is seen in Figure 1, where similar doses of Cas9 were protective in R838S Tg mice. It is important to note that, in the latter setting, the protective effects of editing the mutant R838S transgene likely would have masked any potential negative impact of persistent Cas9 expression.

Optimizing the dose of “hardened” *Gucy2e*

Next, we determined the maximum tolerated dose of “hardened” *Gucy2e*-containing reagents following subretinal injections in the right eyes of *Gucy2e*^{-/-} mice with AAV-*Gucy2e* gRNA-“hardened” *Gucy2e* at doses of 1E8 vg/eye, 3E8 vg/eye, 1E9 vg/eye, and 3E9 vg/eye (Table 1). Left eyes were injected with vehicle alone. *Gucy2e*^{-/-} mice exhibit early loss of cone-mediated function, reduced rod-mediated function, and loss of cone structure beginning at 5 weeks of

age.^{29,30} In previous studies that aimed to treat *Gucy2e*^{-/-} mice with AAV-*Gucy2e* supplementation, significant improvements in cone function and survivability were observed. However, comparatively low levels of functional rescue were seen in the rods.²² For this reason, we classified an effective dose of “hardened” *Gucy2e* as one that rescues cone-mediated function without showing signs of toxic overexpression, as measured through loss of rod photoreceptors (ONL thickness).

Gucy2e^{-/-} mouse eyes injected with 3E8 vg/eye of AAV-*Gucy2e* gRNA-“hardened” *Gucy2e* displayed small but statistically significant improvements in cone-mediated function that emerged at 12 weeks p.i. and were maintained through the duration of the study (Figure 4A). Doses of 1E9 vg/eye and 3E9 vg/eye produced significant improvements in cone function at all time points p.i. relative to vehicle controls. Notably, the magnitude of functional rescue in eyes injected with 3E9 vg/eye was markedly reduced between 12 and 16 weeks p.i., while all other doses led to stable functional improvements. While treatment with 1E9 vg/eye did not lead to any loss of photoreceptors (Figure 4B), there was significant ONL thinning in eyes that received 3E9 vg/eye at 16 weeks p.i. (Figure 4C) relative to vehicle controls. The loss of structure coincided with the loss of photopic b-wave amplitude (Figure 4A) in that dose cohort, suggesting that 3E9 vg/eye is at or above the maximum tolerated dose of the “hardened” *Gucy2e* vector.

In summary, the loss of retinal structure in *Gucy2f*^{-/-} mice injected with 3E9 vg/eye of AAV-*SaCas9* and AAV-*GUCY2D* gRNA-deadGC1 and in *Gucy2e*^{-/-} mice injected with 3E9 vg/eye of AAV-*Gucy2e* gRNA-“hardened” *Gucy2e* led to exclusion of the 3E9 vg/eye dose from future studies. Our “ablate” (CRISPR-Cas9) reagents were capable of achieving biologically meaningful on-target editing at 1E9 vg/eye (Figure 3) in the absence of detectable Cas9-mediated toxicity (Figure S2). Additionally, our “replace” (“hardened” *Gucy2e*) reagent was capable of conferring functional rescue in a RetGC1-null environment in the absence of detectable toxicity emanating from the transgene product at 1E9 vg/eye (Figure 4). Taken together, our results support administration of “ablate and replace” vectors at 1E9 vg/eye.

Development and characterization of the RetGC1 (hR838S, hWT) mouse model

R838S Tg mice harbor multiple copies of the entire human *GUCY2D* gene bearing the R838S mutation randomly inserted into their genome and thus do not accurately recapitulate the genomic landscape of human *CORD6*. For this reason, we designed the RetGC1 (hR838S, hWT) knockin mouse model, which has exon 13 of *Gucy2e*

Figure 2. Effect of the “ablate and replace” system on retinal structure and function following subretinal injection in *Gucy2e*^{+/-}:*Gucy2f*^{-/-} mice

(A) A schematic showing details of the approach. (B) Alignment showing the silent mutations introduced in “hardened” *Gucy2e*. The gRNA sequence (top), sense strand of WT mouse *Gucy2e* (center), and “hardened” sequence (bottom) are shown. Highlighted nucleotides represent a silent mutation introduced in the “hardened” sequence. There are five silent mutations in the gRNA-recognition sequence and two silent mutations in the PAM site. (C) Average scotopic a- and b-wave amplitudes at 20 weeks p.i. (D) Average photopic a- and b-wave amplitudes at 20 weeks p.i. (n = 8–9 animals per treatment). (E) Average ONL thickness in all groups over time. An ANOVA analysis followed by a post-hoc Tukey’s range test was performed on all groups at all time points (C and D) (*p < 0.05). A two-way repeated measure ANOVA followed by a post-hoc Tukey’s range test was used to compare all test groups over time (E). A + R, “ablate and replace” test group, p < 0.05. Significance (*) in (E) is only shown for A + R vs. “ablate only.”

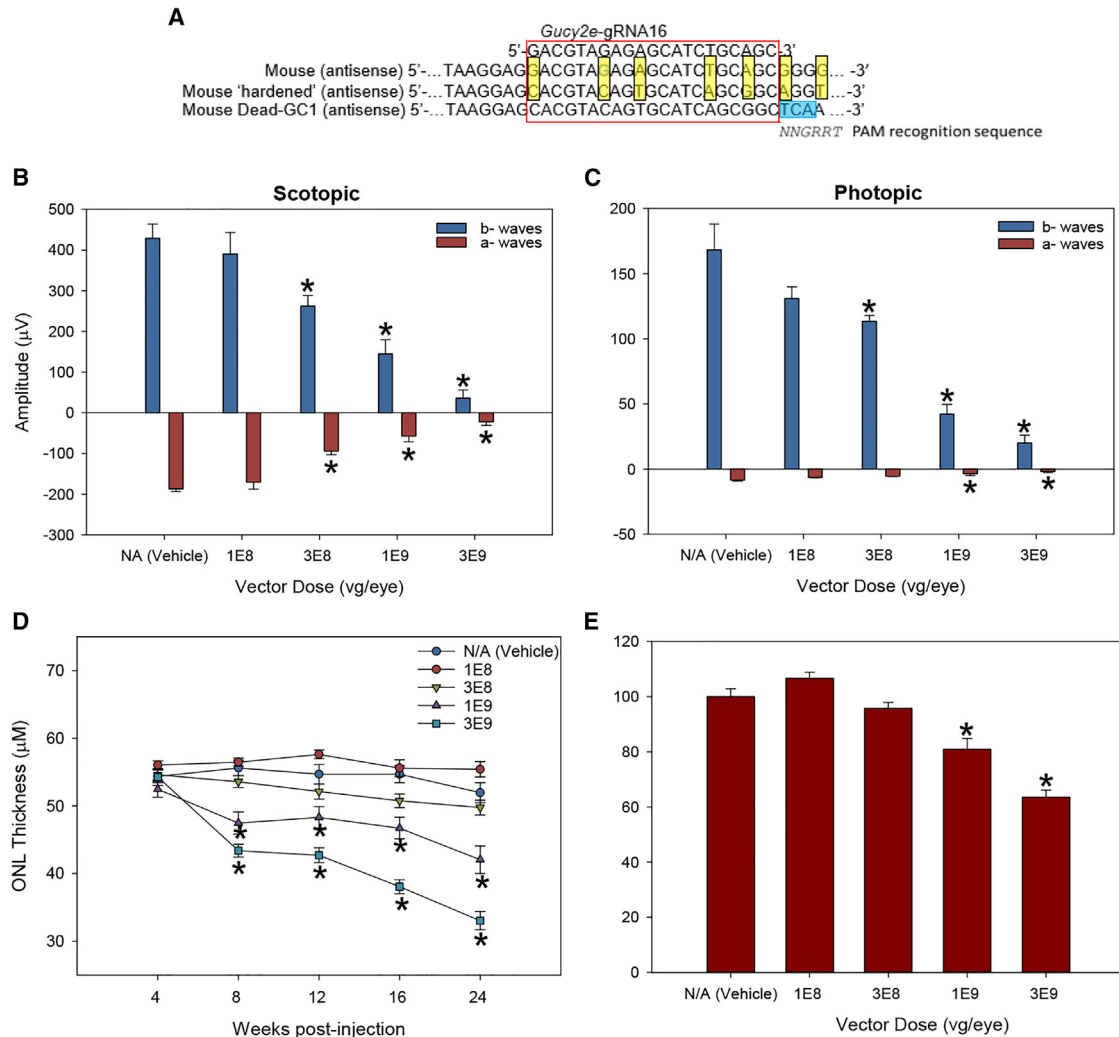


Figure 3. Dose-ranging study performed in *Gucy2f*^{-/-} mice to determine optimal dose of editing reagents (AAV-SaCas9 and AAV-*Gucy2e*-deadGC1) to elicit a physiological response

(A) Alignment showing the dead-GC1 sequence, gRNA sequence, WT *Gucy2e*, and “hardened” *Gucy2e* sequences. Nucleotides highlighted in yellow represent silent mutations introduced in the “hardened” sequence. Nucleotides highlighted in blue represent the stop codon inserted directly adjacent to the gRNA recognition site. (B) Average scotopic a- and b-wave amplitudes at 24 weeks p.i. (C) Average photopic a- and b-wave amplitudes at 24 weeks p.i. (n = 4–7 animals per treatment). (D) Average ONL thickness in vector- vs. vehicle-treated eyes over time from 4 weeks p.i. to 24 weeks p.i., normalized to that seen in vehicle-injected eyes. (E) Percentage of ONL thickness remaining in vector-treated eyes normalized to buffer-injected controls at 24 weeks p.i. An ANOVA analysis followed by a post-hoc Tukey’s range test was performed, comparing each dose with buffer-injected controls (B, C, and E). A two-way repeated-measure ANOVA followed by a post-hoc Tukey’s range test was performed, comparing each dose over time (D). *p < 0.05 relative to buffer-injected controls.

replaced with the corresponding genomic sequence from human *GUCY2D* (Figure 5A). A small portion of exon 14 was replaced, but the replacement did not alter the amino acid sequence of that exon. One allele contains the WT *GUCY2D* sequence (hWT), while the other allele contains the *GUCY2D* sequence bearing the R838S point mutation (hR838S). We characterized the retinal phenotype of the RetGC1 (hR838S, hWT) mice along with RetGC1 (hWT, hWT) mice in which exon 13 of both alleles is replaced with the WT *GUCY2D* sequence (Figure 5A). These “humanized” alleles containing exon 13 from human *GUCY2D* were designed so that the intronic region flanking

exon 13 as well as a small portion of exon 14 consist of the human *GUCY2D* sequence. Fragment insertion was not predicted to affect splicing.

We confirmed expression of our “humanized” alleles by western blot analysis on neural retina lysates from the following mouse lines: (WT) C57BL/6J, RetGC1 (hWT, hWT), RetGC1 (hR838S, hR838S), *Gucy2e*^{+/-}, RetGC1 (hWT, -), RetGC1 (hR838S, -), and *Gucy2e*^{-/-} mice (Figure 5B). We confirmed that RetGC1 expression was equivalent in RetGC1 (hWT, hWT)

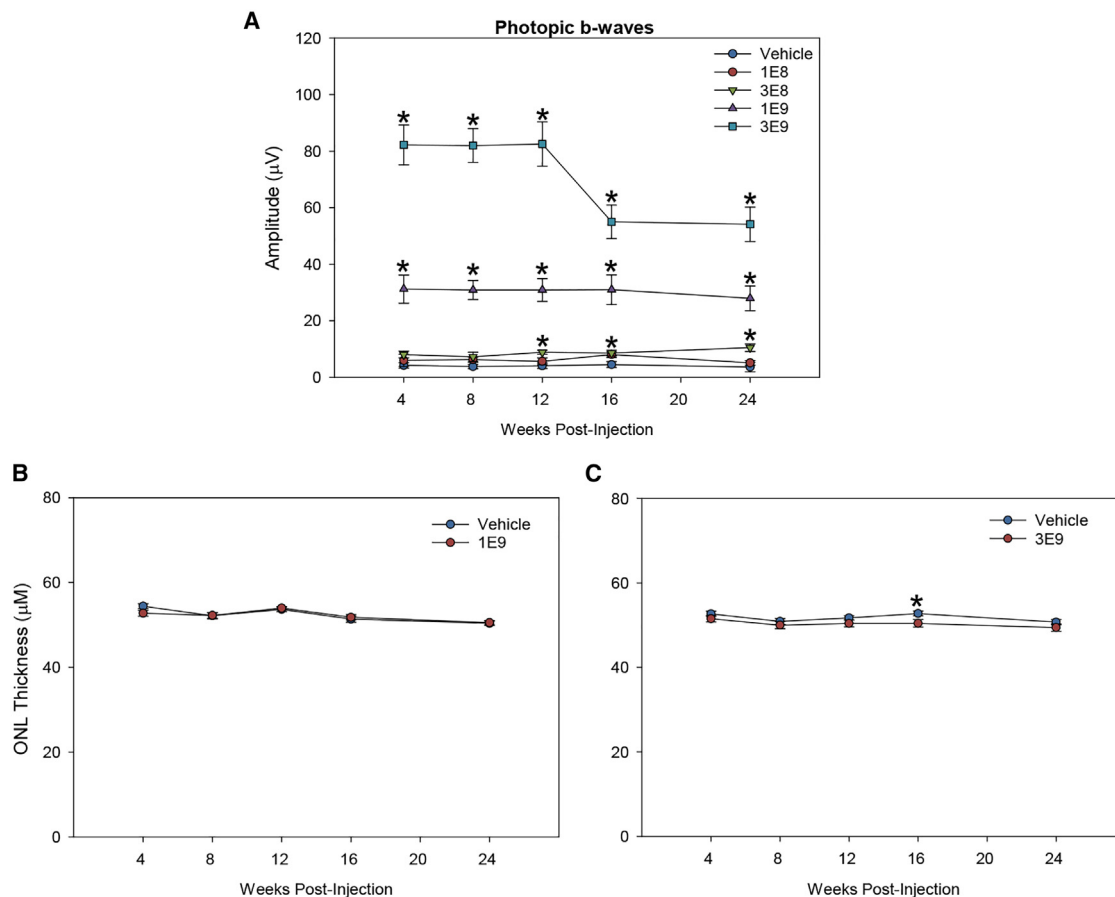


Figure 4. Dose-ranging study performed in *Gucy2e*^{-/-} mice to determine a safe and effective dose of “hardened” *Gucy2e* vector

(A–C) Average photopic b-wave amplitudes (A) and ONL thickness (B and C) over time ($n = 4–7$ mice) in vehicle-injected eyes vs. eyes injected with AAV-*Gucy2e* gRNA-“hardened” *Gucy2e* at four doses. Average ONL thickness data are shown over time in eyes injected with “hardened” *Gucy2e* reagents at a dose of 1E9 vg/eye vs. vehicle-injected eyes (B) and 3E9 vg/eye vs. vehicle-injected eyes (C). A two-way repeated-measure ANOVA followed by a post-hoc Tukey’s range test was used to compare each dose at every time point. * $p < 0.05$ relative to vehicle-injected eyes.

and C57BL/6J (WT) mice (Figure 5C). RetGC1 (hR838S, hR838S) mice express approximately 60% RetGC1 relative to C57BL/6J (WT) mice. This pattern was confirmed at the single-allele level because RetGC1 expression in the RetGC1 (hR838S, –) mouse was approximately 60% that of the heterozygous *Gucy2e*^{+/-} mouse. This suggests that the hR838S allele is expressed at roughly 60% that of the WT *Gucy2e* allele. Despite the lower overall expression, immunohistochemistry (IHC) analysis confirmed that the humanized alleles encode RetGC1 proteins that traffic properly to photoreceptor OSs (Figure S3).

RetGC1 (hR838S, hWT) mice exhibited significantly reduced rod- and cone-function relative to RetGC1 (hWT, hWT) mice at all time points tested (Figures 6A and 6B). No differences in retinal structure or function were observed between RetGC1 (hWT, hWT) and C57BL/6J mice at any time point through 52 weeks of age (data not shown). For this reason, RetGC1 (hWT, hWT) mice served as our “WT controls.” As expected, age-related declines in

ERG amplitudes were observed in both mouse strains. However, loss of rod-mediated function was more pronounced in RetGC1 (hR838S, hWT) mice (75% reduction in average scotopic b-wave maximum amplitudes between 4 and 52 weeks) than in WT controls (50% reduction). Photopic b-wave amplitudes were also significantly reduced in RetGC1 (hR838S, hWT) mice relative to WT controls at all time points (Figure 6B), but both strains exhibited similar rates of functional decline over time (WT mice displayed a 40% decrease in photopic b-wave amplitudes from 4 to 52 weeks of age, while RetGC1 [hR838S, hWT] mice displayed a 35% decrease over the same time frame).

Additional parameters of the ERG waveform (besides the b-wave amplitude) can point to signs of photoreceptor dysfunction. In cone-rod dystrophies, altered photopic ERG waveform kinetics can also be used to diagnose functional impairment.³¹ RetGC1 (hR838S, hWT) mice exhibit notably delayed photopic waveform kinetics relative to RetGC1 (hWT, hWT) mice (Figure S4A). We

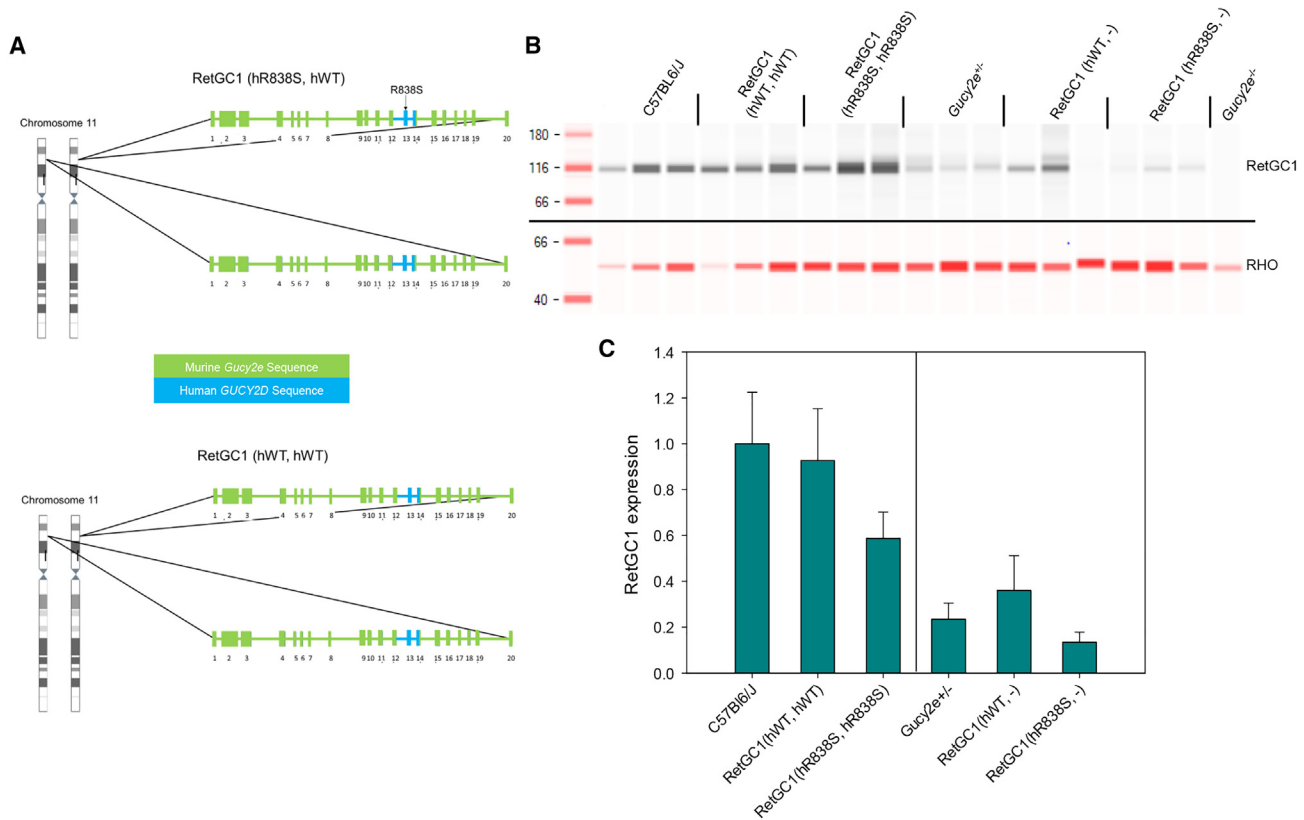


Figure 5. Creation and characterization of retGC1 expression in a novel knockin mouse model of CORD6

(A) Schematic showing *Gucy2e* alleles in the RetGC1 (hR838S, hWT) (top) and RetGC1 (hWT, hWT) (bottom) mouse models. The thin lines within the gene represent the intronic sequence, while thicker blocks represent the exonic sequence. Green portions of the gene represent the murine *Gucy2e* sequence, while blue portions of the gene represent the human *GUCY2D* sequence. The location of the R838S mutation is indicated with an arrow. (B) RetGC1 expression in the chemiluminescent channel (top) and rhodopsin (RHO) in the NIR channel (bottom) of a western blot generated via ProteinSimple Jess. (C) RetGC1 protein expression from five mouse lines is expressed relative to WT expression (C57BL/6J). A one-way ANOVA followed by a post-hoc Tukey's range test was performed to compare retGC1 expression in RetGC1 (hWT, hWT) and RetGC1 (hR838S, hR838S) with WT levels as well as to compare RetGC1 expression in the RetGC1 (hWT, KO) and RetGC1 (hR838S, KO) mice with that of *Gucy2e*^{+/+} mice ($p < 0.05$).

quantified five separate measures of wave kinetics to quantify trends in the photopic waveforms for each respective mouse line. The “latency” of the a- and b-waves are defined as the time from stimulus onset to the beginning of the wave. The a- and b-wave “implicit times” are defined as the time from stimulus onset to waveform peak. The “time to baseline” measurement refers to the time between stimulus onset and return of the b-wave to pre-stimulus levels. The “time to baseline” measurement was not shown to correlate with b-wave amplitude for either mouse line. Photopic a-wave latencies increased with age in both mouse models and, beginning at 28 weeks of age, were significantly longer in RetGC1 (hR838S, hWT) mice relative to WT controls (Figure S4B). Photopic a-wave implicit times were significantly longer in RetGC1 (hR838S, hWT) mice relative to WT controls at some but not all time points (Figure S4C). Photopic b-wave measurements (latency, implicit time, and return to baseline) revealed significant delays in RetGC1 (hR838S, hWT) mice relative to WT controls at all time points. (Figures S4D–S4F). These results

further indicate that the mutant R838S cyclase leads to aberrant cone function in RetGC1 (hR838S, hWT) mice.

RetGC1 (hR838S, hWT) mice exhibited significantly reduced average ONL thickness compared with RetGC1 (hWT, hWT) mice as early as 4 weeks of age (Figure 6C). Loss of ONL continued over the lifetime of the mouse, decreasing by 51% from 4 to 52 weeks of age. Mouse retinas are predominantly composed of rods, and thus a decrease in ONL thickness primarily indicates rod degeneration. Loss of structure and function were contemporaneous in RetGC1 (hR838S, hWT) mice (Figure 6A). Because cone cell loss is not readily evident via optical coherence tomography (OCT), we conducted a cone survivability assay using immunostained retinal whole mounts from RetGC1 (hR838S, hWT) and WT control mice. Retinas from 52-week-old mice were stained with a cone cell marker, and punctate cone staining was quantified (Figure S5). There was no significant difference in the number of cones in RetGC1 (hR838S, hWT) mice relative to WT controls at 52 weeks

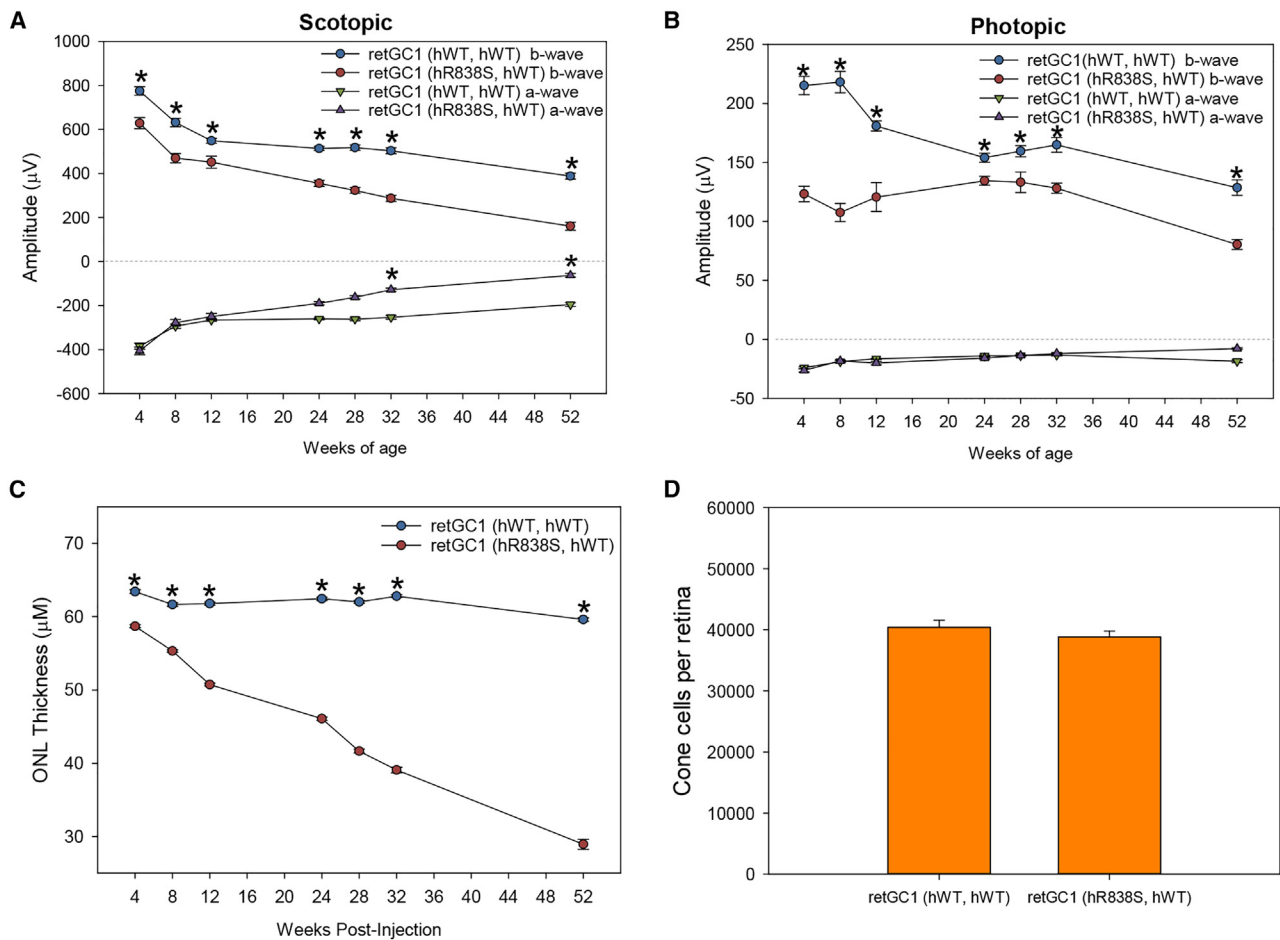


Figure 6. Characterization of retinal structure and function in the RetGC1 (hR838S, hWT) mouse model

(A and B) Average scotopic (A) and photopic (B) a- and b-wave amplitudes over time in RetGC1 (hR838S, hWT) mice (n = 10) vs. RetGC1 (hWT, hWT) controls (n = 10). (C) Average ONL thickness over time in RetGC1(hR838S, hWT) vs. RetGC1 (hWT, hWT) controls. A two-way repeated-measure ANOVA followed by a post-hoc Tukey’s range test was performed comparing a- and b-wave amplitudes between groups over time (*p < 0.05). (D) Cone cell counts from RetGC1 (hWT, hWT) (n = 5) and RetGC1 (hR838S, hWT) (n = 7) mouse retinas at 52 weeks of age. A Student’s t test was used to determine significance between the two test groups (*p < 0.05).

of age (Figure 6D). Despite their aberrant function (reduced b-wave amplitudes and delayed response kinetics), cones remain structurally intact in RetGC1 (hR838S, hWT) mice.

Validating the ‘ablate and replace’ approach in the RetGC1 (hR838S, hWT) mouse model of CORD6

RetGC1 (hR838S, hWT) mice are the first available model to accurately replicate the genetic landscape of CORD6. Their underlying mutation is associated with retinal dysfunction and rod degeneration, providing outcome measures against which we could measure efficacy of the “ablate and replace” system. Because of the early-onset phenotype seen in these mice (detectable as early as 4 weeks of age), all injections were performed at weaning (~post-natal day 21 [P21]). Based on results of the dose-ranging studies described above, “ablate and replace” vectors were each injected at a dose of 1E9 vg/eye. RetGC1 (hWT,

hWT) mice were bilaterally injected with vehicle as a control (Table 1). A schematic showing injection details is shown in Figure 7A.

RetGC1 (hR838S, hWT) mouse eyes treated with “ablate and replace” vectors (AAV.SPR-hGRK1-SaCas9 + AAV.SPR-U6-Gucy2e gRNA-hGRK1-“hardened” Gucy2e) had increased scotopic b-wave amplitudes relative to vehicle-injected control eyes for at least 24 weeks p.i. This achieved statistical significance by 24 weeks p.i. (Figure 7B). At that point, there was no significant difference in scotopic b-wave amplitudes between treated RetGC1 (hR838S, hWT) mice and WT controls. Functional improvements were more obvious at lower stimulus intensities. At 2.5 candela per meter squared (cd s/m²) (akin to lighting 15 min after sunset), significant functional improvements in treated eyes vs. contralateral controls took between 20 and 24 weeks to emerge, while at 0.025 cd s/m² (dimmer condition akin to full moonlight), treated eyes displayed significant functional improvements as early as 8 weeks p.i.

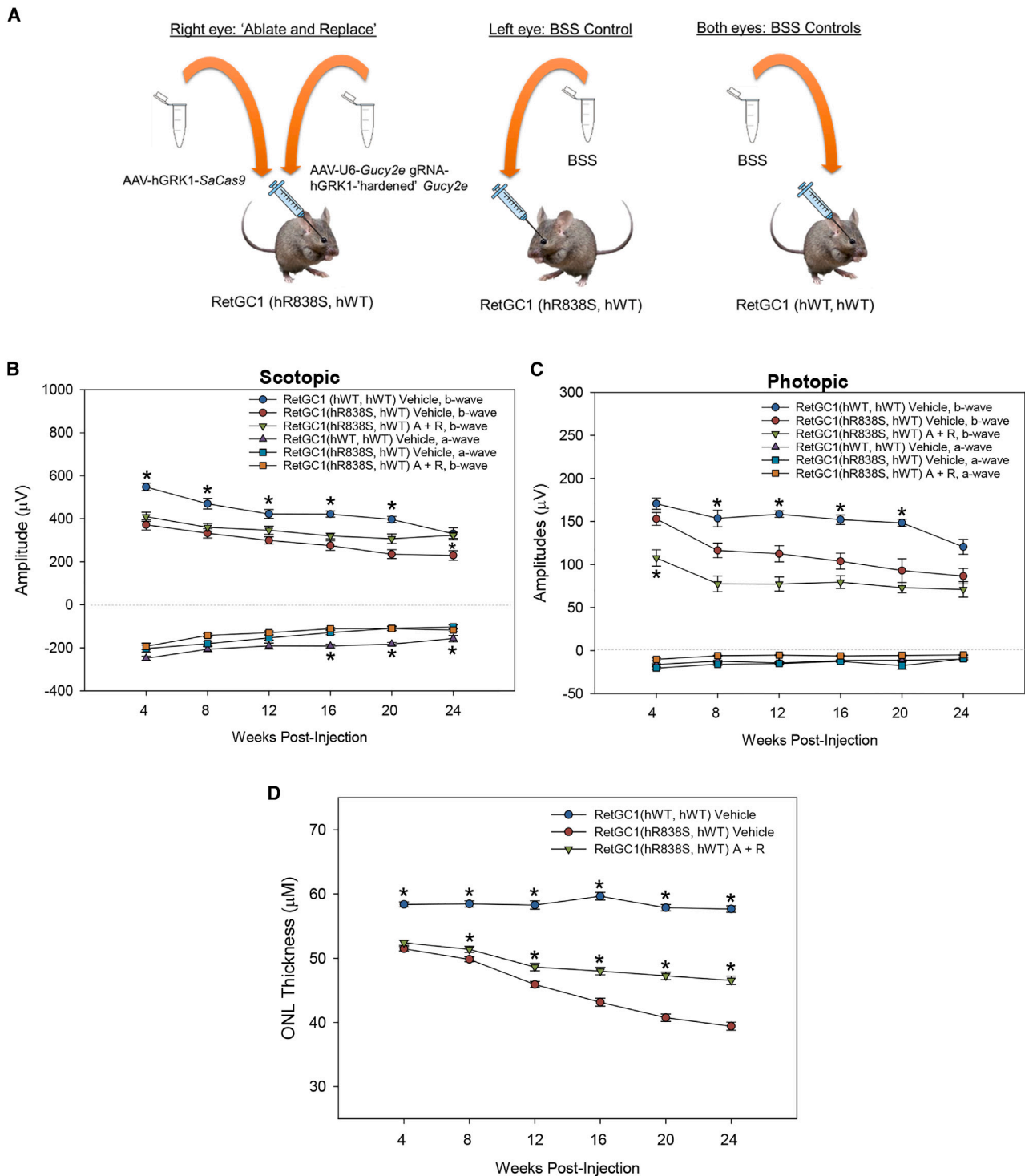


Figure 7. Validation of the A + R approach in the RetGC1(hR838S, hWT) mouse model of CORD6

(A) Schematic illustrating details of the approach. (B and C) Average scotopic (B) and photopic (C) a- and b-wave amplitudes in RetGC1(hR838S, hWT) eyes injected with AAV.SPR-hGRK1-SaCas9 + AAV.SPR-U6-Gucy2e gRNA-hGRK1-"hardened" Gucy2e (here labeled "A + R") (n = 8), contralateral eyes injected with vehicle (n = 8), and RetGC1(hWT, hWT) eyes injected with vehicle (n = 12). (D) Average ONL thickness over time in RetGC1(hR838S, hWT) eyes injected with A + R, contralateral eyes injected with vehicle, and RetGC1(hWT, hWT) eyes injected with vehicle. A two-way repeated measure ANOVA followed by a post-hoc Tukey's range test was performed to compare

(legend continued on next page)

(Figure S6). No significant improvements in photopic ERG were observed in RetGC1 (hR838S, hWT) mouse eyes treated with the “ablate and replace” vectors. In fact, treated eyes displayed slightly reduced photopic b-waves relative to vehicle-injected controls at multiple time points, but these differences were never significant (Figure 7C).

As mentioned previously, the photopic waveform kinetics of RetGC1 (hR838S, hWT) mice are abnormal relative to those of RetGC1 (hWT, hWT) mice (Figure S5). While significant improvements in photopic b-wave amplitudes were not achieved with our “ablate and replace” approach, we did observe partial correction of waveform kinetics in treated RetGC1 (hR838S, hWT) mice under photopic conditions (Figure S7A). Reductions (improvements) in b-wave implicit times and time-to-baseline were seen RetGC1 (hR838S, hWT) mice treated with “ablate and replace” vectors relative to vehicle-injected controls (Figures S7E and S7F). Next we asked whether improvements in photopic waveform kinetics translated to gains in useful vision. Optokinetic reflex testing performed under photopic conditions showed that treated eyes of RetGC1 (hR838S, hWT) mice had higher spatial frequency thresholds than vehicle-injected controls, although this difference was not statistically significant. There was no difference in the spatial frequency threshold of RetGC1 (hR838S, hWT) treated eyes and RetGC1 (hWT, hWT) eyes (Figure S8). The absence of a difference between RetGC1 (hR838S, hWT) mice and the WT controls indicates that performing optokinetic reflex testing (OKN) in this model is of limited value.

Finally, we evaluated the impact of the “ablate and replace” approach on retinal structure. Treated RetGC1 (hR838S, hWT) eyes exhibited significant and stable preservation of ONL thickness relative to vehicle-injected controls beginning at 8 weeks p.i. and continuing to 24 weeks p.i. (Figure 7D). However, the ONL was not maintained at the same thickness as seen in WT controls. Taken together, we demonstrated that the “ablate and replace” system was capable of partially preserving photoreceptor structure and function in the RetGC1 (hR838S, hWT) mouse model of CORD6. UDiTaS analysis in 6 neural retinas injected with the “ablate and replace” reagents revealed an average on-target editing rate of 24% with a maximum editing rate of 35%. In 4 of 6 retinas, editing was between 30% and 35%. The other two retinas had between 0% and 10% editing, suggestive of less efficient subretinal injections. As before, this underrepresents the total percentage of edited photoreceptors.

DISCUSSION

In this study, we employed multiple AAV-CRISPR-Cas9-based approaches and mouse models to develop a potential treatment for *GUCY2D*-associated CORD6. First, we established a proof of concept that disrupting the early coding sequence to “ablate” expression of mutant R838S *GUCY2D* was therapeutic in a Tg mouse model. R838S Tg

mice harbor multiple copies of the R838S *GUCY2D* coding sequence under control of the rhodopsin promoter inserted randomly into their genome and, like CORD6 patients, display early-onset retinal degeneration. Ablation of the mutant transgene via AAV-CRISPR-Cas9 successfully halted disease progression. Limitations of the R838S Tg mouse, however, include the unknown number of mutant transgene copies inserted randomly into the genome (editing at the natural genomic location cannot be assessed) and their endogenous *Gucy2e* expression. The species specificity of our gRNA (directed against *GUCY2D*) leaves endogenous *Gucy2e* intact. As a result, even successfully edited photoreceptors in R838S Tg mice retain RetGC1 function, which is inconsistent with the human condition. For these reasons, we developed the RetGC1 (hR838S, hWT) knockin mouse model to ensure evaluation of editing at the natural genomic location in a model where the numbers of WT and mutant alleles were balanced and physiologically relevant. It was only in this model of CORD6 that the “ablate and replace” system could be tested reliably.

RetGC1 (hR838S, hWT) mice incorporate the *GUCY2D* sequence from the critical exon 13, with one allele harboring the R838S mutation and the other allele containing the WT human sequence. They exhibit reduced cone function and aberrant cone-mediated ERG waveform kinetics but no loss of cone photoreceptors. In contrast, rod photoreceptors are dysfunctional and degenerate progressively. This suggests that the R838S mutant cyclase more negatively impacts rod photoreceptors in the context of the mouse retina. This differs from the CORD6 patient phenotype, which is characterized by early-onset cone dysfunction/degeneration and variable rod involvement.³²

Why does the R838S mutant cyclase more negatively impact rods in the mouse retina? Perhaps aberrant activation of RetGC1 in the ISs, which is thought to bring about photoreceptor degeneration, occurs at similar rates in rods and cones. It is possible that rod-derived cone viability factor (RdCVF), or something similar/rod derived, protects cone photoreceptors from degeneration in RetGC1 (hR838S, hWT) mice. RdCVF, a protein secreted by rods, is known to protect cone cells from death in humans and mice.³³ It is possible that the unique retinal morphology of the human vs. mouse retina accounts for the phenotypic differences we observed. The cone-exclusive human fovea potentially has low/no access to viability factor because of its seclusion from rod photoreceptors. In contrast, mouse cones, which are evenly dispersed among rods throughout the retina, may survive because of an abundance of viability factor secreted by adjacent rods despite an accumulation of mutant RetGC1 in their OSs. Despite their structural maintenance, cone photoreceptors in RetGC1 (hR838S, hWT) mice are dysfunctional, a result likely owed to the buildup of the mutant cyclase with altered calcium sensitivity in the OSs of these cells.²⁰ We have begun generating the “all-cone” *Nrl*^{-/-};hR838S mouse to investigate whether the impact of

groups over time (*p < 0.05). In (B) and (C), significance markers (*) located adjacent to the RetGC1(hWT, hWT) vehicle data indicate a significant difference relative to all other groups. All other markers (*) represent significance between A + R vs. vehicle-injected RetGC1(hR838S, hWT) mice. In (D), significance markers (*) located above the RetGC1(hWT, hWT) vehicle data indicate a significant difference relative to all other groups. Significance (*) markers above RetGC1(hR838S, hWT) A + R data indicate a significant difference relative to RetGC1(hR838S, hWT) mice treated with vehicle alone.

the mutant cyclase would be different in a cone-dominant retina. It may also be informative to evaluate the “ablate and replace” approach in *CORD6*-patient derived retinal organoids.

Despite these phenotypic differences, administration of “ablate and replace” vectors in RetGC1 (hR838S, hWT) mice at the optimal dose of 1E9 vg/eye led to significant preservation of ONL thickness, significant preservation of rod-mediated function, and partial correction of cone-mediated ERG waveform kinetics. These results provide critical preclinical support for development of a *CORD6* treatment. One shortcoming of the RetGC1 (hR838S, hWT) mouse model is that it is only “partially humanized” (it only contains a human sequence in exons 13/14) and thus still relies on a gRNA targeted to the early murine coding sequence to ablate expression. Future directions of this study include creation of a double knockin mouse containing human *GUCY2D* from exon 13 (the site of mutation) and exon 4 (the *GUCY2D* gRNA recognition sequence). Successful treatment of this double knockin mouse with an AAV-CRISPR-Cas9-based “ablate and replace” system targeting the human locus would provide additional support for clinical development of this approach for *CORD6*.

MATERIALS AND METHODS

CRISPR-Cas9 system design and optimization

Design and optimization of CRISPR-Cas9 reagents that target murine *Gucy2e* and human *GUCY2D* have been published previously.¹⁹ In brief, gRNAs were designed using Godot, a custom gRNA design software based on the publicly available software Cas-OFFinder, to target early coding regions of *Gucy2e* and *GUCY2D*.³⁴ Prioritization was given to gRNAs that were species specific. Transfections were performed *in vitro* using polyethylenimine (PEI) and a plasmid containing *Staphylococcus aureus* Cas9 (*SaCas9*) driven by the cytomegalovirus (CMV) promoter and linear DNA expressing gRNAs driven by the U6 promoter. Murine *Gucy2e*-targeting gRNAs were transfected into NIH3T3 cells (originally obtained from Dr. Nicolas Muzyczka, University of Florida), while human *GUCY2D*-targeting gRNAs were transfected into HEK293 cells (ATCC). Three days post transfection, cells were harvested, genomic DNA was isolated (Agencourt DNAdvance kit, Beckman Coulter), and editing rates were determined using PCR followed by a T7 endonuclease assay (New England Biolabs). The gRNAs that most effectively edited *Gucy2e* and *GUCY2D* while maintaining species specificity were carried forward.

Experimental animals

The Tg(Rho-GUCY2D**R838S*)362Amd mouse model, commonly known as the *R838S* Tg slow mouse model (and here referred to as “*R838S* Tg”) in the C57BL6 background has been described previously^{11,20} and provided by the Dizhoor lab (Salus University). Mice were bred to homozygosity and then crossed with WT C57BL/6J mice, yielding the heterozygous mice used in experiments. RetGC1 knockout (*Gucy2e*^{-/-}) mice on the 129/SvJ background originating from the Garbers lab (University of Texas Southwest Medical Center) have been described previously.²⁹ Homozygosity was maintained

through inbreeding, and heterozygous *Gucy2e*^{+/-} mice were produced by breeding with WT C57BL/6J mice, creating a mixed background. RetGC2, an isozyme of RetGC1, is encoded by X-linked *Gucy2f* and is expressed exclusively in rods.^{10,29,35} The RetGC2 knockout (*Gucy2f*^{-/-}) mouse line has been described previously²⁶ and was generously provided by the Baehr lab (University of Utah). GCdko mice have been described previously.²⁶ These mice were bred with *Gucy2f*^{-/-} knockout animals to yield *Gucy2e*^{+/-}:*Gucy2f*^{-/-} mice, which contain a single functional copy of *Gucy2e*. RetGC1 (hR838S, hR838S) and RetGC1 (hWT, hWT) mice were generated in collaboration with The Jackson Laboratory. RetGC1 (hR838S, hR838S) mice contain exon 13 of human *GUCY2D-R838S* inserted in place of murine *Gucy2e* exon 13. RetGC1 (hWT, hWT) mice contain WT exon 13 of *GUCY2D* inserted in place of the murine *Gucy2e* exon 13. C57BL/6J mouse zygotes were harvested 12 h post coitum, and pronuclear microinjection of Cas9 in complex with two separate gRNAs and a DNA donor sequence was performed. One gRNA targeted the early coding sequence of exon 13, while the second targeted the early coding sequence of exon 14. Guides were selected based on their low likelihood to induce off-target editing, as determined by the CRISPOR online software. The WT DNA template contained the *GUCY2D* sequence spanning from exon 13 through the early coding sequence of exon 14. The *R838S* DNA template sequence contained a C-to-A transversion at *GUCY2D* position 2586 as well as three silent mutations in the early coding sequence of exon 14 that aid in identification of the locus when sequenced. Edited embryos were implanted into pseudopregnant C57BL/6J females, and progeny were screened for the desired genotype at weaning. Mice were bred to homozygosity and maintained at the University of Florida. RetGC1 (hWT, hWT) females were crossed with RetGC1 (hR838S, hR838S) males to produce RetGC1 (hR838S, hWT) mice. RetGC1 (hR838S, hR838S) mice were bred with *Gucy2e*^{-/-} mice to yield RetGC1 (hR838S, -) mice. Homozygous RetGC1 (hWT, hWT) mice were bred with *Gucy2e*^{-/-} mice to yield RetGC1 (hWT, -) mice.

Mice were bred, maintained, and housed at the University of Florida’s Health Science Center Animal Care Services Facility. Food and water were available *ad libitum*, and mice were maintained in a 12 h/12 h light/dark cycle. The University of Florida’s Institutional Animal Care and Use Committee approved all animal work, which we performed in accordance with the Association for Research in Vision and Ophthalmology Statement for the Use of Animals in Ophthalmic and Vision Research.

AAV vectors

All AAV vector plasmids were constructed using standard ligation methods. *SaCas9* driven by the human rhodopsin kinase (hGRK1) promoter was inserted into an AAV inverted terminal repeat (ITR)-containing plasmid.^{19,36} A second plasmid contained the *GUCY2D* gRNA driven by the U6 promoter upstream of a CRISPR-Cas9-resistant (“hardened”) cDNA copy of *Gucy2e* driven by the hGRK1 promoter. The “hardened” *Gucy2e* construct harbors five silent mutations in the gRNA-recognizing portion of the coding sequence and two silent mutations in the PAM sequence, all of which

were added using site-directed mutagenesis.²³ The “ablate only” control plasmid was constructed by replacing the “hardened” *Gucy2e* with green fluorescent protein (GFP). A non-functional “deadGC1” transgene was created by introducing a stop codon directly adjacent to the would-be gRNA recognition site of “hardened” *Gucy2e*. The “toxicity control” was created by swapping the *GUCY2D*-targeting gRNA with the species non-specific *Gucy2e*-targeting gRNA (because Cas9 unpaired from gRNA can negatively impact transduced cells, this ensured pairing of Cas9 with gRNA in the absence of editing). For editing experiments in R838S Tg mice, the gRNA targeting the *GUCY2D* early coding sequence was replaced by the *Gucy2e* gRNA in the “ablate only” plasmid.

All vectors were packaged in AAV.SPR using a standard plasmid-based transfection method in adherent HEK293 cells, purified by iodixanol density gradient centrifugation followed by buffer exchange and concentration, and titered by dot blot in the Powell Gene Therapy Vector Core at the University of Florida according to previously published methods.³⁷ Titers were confirmed by qPCR targeting the bovine growth hormone polyadenylation signal (bgh-poly[A]) using the following primers: bgh-poly(A) forward (5'-CCATCTGTTGT TGGCCCTC-3') and bgh-poly(A) reverse (5'-GACAATGCGATG CAATTTCC-3'). These primers produce an amplicon of 199 bp using the following PCR conditions: (1) initial denaturation at 95°C for 10 min; (2) 34 cycles of 95°C denaturation for 30 s, 52°C annealing for 30 s, and 72°C elongation for 30 s; and (3) final elongation at 72°C for 1 min. Vectors were tested for the presence of endotoxin and were determined to be below the acceptable limit of 5 endotoxin units (EU)/mL. Vectors were diluted using BSS supplemented with 0.014% Tween to the desired experimental concentrations.

Subretinal injections

Mice were subretinally injected between P15 and P40, as described previously.³⁸ Eyes were dilated using 1% tropicamide (Bausch+Lomb) and 2.5% phenylephrine (Paragon Biotek) applied 15 min and 5 min before sedation, respectively. Sedation was performed with ketamine (100 mg/kg) and xylazine (10 mg/kg) by intraperitoneal injection. A small corneal hole was made to enable a *trans*-corneal subretinal injection using a Hamilton syringe attached to a 33G blunt needle. For all animals, 1 μ L of the appropriate test article was delivered, and approximately equal numbers of males and females were used. A summary of mouse injections is provided in Table 1.

ERG analysis

Mice were dark adapted for a minimum of 12 h prior to testing. Pupils were dilated, and mice were sedated as described above. Hypromellose solution (2.5%, Akorn) was applied to eyes for hydration, and full-field electroretinograms were recorded using the Celeris D430 (Diagnosys) according to previously described methods.¹⁹ Briefly, scotopic electroretinograms were recorded at interstimulus intervals of 30 s and at stimulus light intensities of 0.025 cds/m², 0.25 cds/m², and 2.5 cds/m². At each light intensity, five measurements were averaged, yielding an average waveform. Light adaptation was carried out with a continual white light stimulus at 5 cds/m² for 5 min. Photopic responses were re-

corded at stimulus light intensities of 1.25 cds/m², 5 cds/m², 10 cds/m², and 25 cds/m². At each light intensity, 50 responses with an interstimulus interval of 0.4 s were averaged. Scotopic and photopic a-wave amplitudes representing photoreceptor hyperpolarization and b-wave amplitudes representing higher-order neuron depolarization were quantified and averaged for each test group. For experiments involving RetGC1 (hR838S, hWT) and RetGC1 (hWT, hWT) mice, waveform kinetics were also analyzed. These included implicit times, a-wave latency, b-wave latency, and “time to baseline.” Implicit times refer to the amount of time required from stimulus onset to either the a- or b-wave peak amplitude. a-wave latency refers to the amount of time from stimulus onset to the beginning of a detectable response. b-wave latency refers to the amount of time from stimulus onset to the time when the depolarizing response rises above baseline.³⁹ “Time to baseline” refers to the amount of time between the b-wave peak and its return to baseline. For all longitudinal measurements, a two-way repeated-measure ANOVA (analysis of variance) followed by a post-hoc Tukey’s range test was used. For all studies involving more than two test groups, a one-way ANOVA followed by a post-hoc Tukey’s range test was performed. For all tests comparing two groups at a single time point, Student’s t tests were used to determine differences between groups. Significance is defined as $p < 0.05$.

OCT

Prior to OCT measurements, mouse pupils were dilated using tropicamide (1%) and phenylephrine (2.5%). Hypromellose solution (2.5%) was applied to maintain hydration. Following sedation, cross-sectional retinal images were obtained using the spectral domain OCT system (Bioptigen, Durham, NC). ONL thickness was measured as described previously using the InVivoView commercial software (Bioptigen).⁴⁰ For each OCT scan, one region 3 mm above the optic nerve meridian, one region 3 mm below the optic nerve meridian, and one region at the optic nerve meridian were selected. At each meridian, 3 measurements were taken 3 mm apart, creating a grid system of measurements centered at the optic nerve. Each scan yielded 8 measurements per eye because ONL thickness cannot be measured at the optic nerve head. ONL thickness was measured from the outer plexiform layer to the external limiting membrane. ONL thickness measurements from all mice in each test group were averaged. For all longitudinal measurements, a two-way repeated-measure ANOVA followed by a post-hoc Tukey’s range test was used. For all studies involving more than two test groups, a one-way ANOVA followed by a post-hoc Tukey’s range test was performed. For all tests comparing two groups at a single time point, Student’s t tests were used to determine differences between groups. Significance is defined as $p < 0.05$.

Visually guided behavior (optokinetic reflex)

Photopic spatial frequency thresholds, markers of cone-mediated visually guided behavior, were measured using the Optomotry system (Cerebral Mechanics) according to previously established methods.⁴¹ Average thresholds were determined for each test group, and one-way ANOVA followed by a post-hoc Tukey’s range test was used to

analyze differences between groups. Statistical significance was defined as $p < 0.05$.

Western blotting

We collected neural retinas from RetGC1 (hR838S, hR838S), RetGC1 (hWT, hWT), RetGC1 (hR838S,-), RetGC1 (hWT,-), *Gucy2e*^{+/-}, and *Gucy2e*^{-/-} mice. Samples were homogenized in radioimmuno-precipitation assay (RIPA) buffer (Thermo Scientific, 89901), and protein concentrations were determined using the bicinchoninic acid (BCA) assay (Thermo Scientific, 23225). Samples were run in triplicate using the Jess Automated Western Blot System (ProteinSimple, San Jose, CA, USA) following the standard 12-230-kDa separation module procedure (ProteinSimple, SM-FL001). Protein was diluted to a concentration of 0.5 $\mu\text{g}/\mu\text{L}$ in 0.1 \times sample buffer (ProteinSimple, 042-195). Following sample loading, running, and ultraviolet immobilization, immunoprob- ing was performed using an anti-RetGC1 mouse monoclonal antibody (Santa Cruz Biotechnology, sc-376217) diluted 1:25 in ProteinSimple diluent 2 (042-203) and an anti-visual arrestin rabbit polyclonal antibody (Thermo Fisher Scientific, PA5-116378) diluted 1:200. Secondary immunoprob- ing was performed using anti-mouse horseradish peroxidase (HRP) antibody (ProteinSimple, 042-205) and anti-rabbit near infrared (NIR) antibody (ProteinSimple, 043-819). Quantifica- tion was performed using the commercial Compass software (ProteinSimple), with RetGC1 expression for each genotype calcu- lated relative to visual arrestin expression as a loading control.

On-target editing analysis

Neural retinas were collected from 36-week-old Tg mice treated with doses of 3E9 vg/eye and 3E10 vg/eye. DNA was isolated using the DNeasy Blood and Tissue Kit (QIAGEN, 69506). On-target editing rates were determined using the UDiTaS system according to previously established methods.²¹ Neural retinas were collected from 28-week-old RetGC1 (hR838S, hWT) mice and were analyzed using the UDiTaS sys- tem as before. The amplification primer was placed in an intronic region so that there was no detection of exogenous, “hardened” *Gucy2e*.

Tissue preparation and immunohistochemistry

Mice were sacrificed between 1 and 12 months of age. Eyes were enucleated and fixed in 4% paraformaldehyde (PFA) for 12 h, and eyecups were dissected and prepared for sectioning according to es- tablished methods.²² Eyes were oriented vertically in optimal cutting temperature medium (Sakura, 4583) and flash frozen, and then cry- osections (12 microns) were cut and fixed to microscope slides. Sec- tions were permeabilized using 5% Triton X-100 detergent in PBS and blocked using 1% bovine serum albumin (BSA) in PBS. Cryosections were immunostained overnight with either anti-RetGC1 rabbit poly- clonal antibody (generously provided by Dr. Alex Dizhoor, Salus Uni- versity) or anti-rhodopsin mouse polyclonal antibody (generously provided by Dr. Clay Smith, University of Florida) diluted 1:500 in PBS containing 0.3% Triton X-100 and 1% BSA. Immunoglobulin G (IgG) secondary antibody Alexa Fluor 488 (Thermo Fisher, Z25302) or Alexa Fluor 594 (Thermo Fisher, A11032) diluted 1:500 in PBS was added for 1 h at room temperature. Sections were counter-

stained with DAPI diluted 1:10,000 for 5 min at room temperature. Images were taken using the All-in-One Fluorescence Microscope (Keyence, Itasca, IL, USA). Gain and exposure settings remained con- stant across sections from the same experiment.

Immunohistochemistry of retinal whole mounts and cone cell counting

Mice were sacrificed at 12 months of age. Eyes were enucleated and fixed in 4% PFA for 12 h. Eyes were dissected, lenses were removed, and eyecups were placed in 4% PFA overnight as before. The choroid and retinal pigment epithelium (RPE) were carefully removed to yield the neural retina, which was cut in four equidistant locations (from the edge of the retina toward the optic nerve) to allow eventual flat- tening on a slide. Retinas were permeabilized in 5% Triton X-100 in PBS for 24 h and blocked in 1% BSA in PBS for 24 h. Immunostain- ing was carried out by adding the retinas directly into solution con- taining anti-cone arrestin antibody (Millipore, AB15282) diluted 1:100 in 0.3% Triton X-100 and 1% BSA for 48 h. Retinas were then washed and placed into solution containing IgG secondary anti- body Alexa Fluor 488 (Thermo Fisher, Z25302) diluted 1:500 in PBS for 24 h. Retinas were then mounted on a microscope slide and imaged using the All-in-One Fluorescence Microscope (Keyence). Gain/exposure settings were optimized for each individual retina to obtain the clearest view of punctate cone photoreceptor staining. Cone counting was carried out using the commercial software ImageJ (National Institutes of Health).⁴² Each retina was divided into quad- rants, where settings were optimized to ensure that each site of punctate fluorescence was counted. The total number of punctate staining sites (cones) was added together from all quadrants to yield the total number of cones. For each test group, the number of cones per retina was averaged. t tests were used to determine differences between groups, with significance defined as $p < 0.05$.

DATA AVAILABILITY

Materials and protocols will be distributed to qualified scientific re- searchers for non-commercial, academic purposes.

SUPPLEMENTAL INFORMATION

Supplemental information can be found online at <https://doi.org/10.1016/j.omtm.2023.05.020>.

ACKNOWLEDGMENTS

This work was supported by R01EY028968 (to S.E.B.). We would like to thank Alex Dizhoor at Salus University for donation of the R838S Tg mouse line and Morgan Maeder and Georgia Giannoukos at Edi- tas Medicine for help with reagent generation and editing analysis, respectively.

AUTHOR CONTRIBUTIONS

Conceptualization, S.E.B. and S.L.B.; funding acquisition, S.E.B.; writing – original draft, R.W.M.; writing – review & editing, S.E.B. and R.W.M.; data curation, R.W.M., K.R.C., K.T.M., S.M.C., A.d.I.C., D.F., and E.X.; formal analysis, R.W.M., K.R.C., K.T.M., and S.E.B.

DECLARATION OF INTERESTS

S.E.B. and S.L.B. are cofounders of Atsena Therapeutics, a company with related interests. They are recipients of research funding from Atsena Therapeutics.

REFERENCES

- Gill, J.S., Georgiou, M., Kalitzeos, A., Moore, A.T., and Michaelides, M. (2019). Progressive cone and cone-rod dystrophies: clinical features, molecular genetics and prospects for therapy. *Br. J. Ophthalmol.* *103*, 711–720. <https://doi.org/10.1136/bjophthalmol-2018-313278>.
- Smith, M., Whittock, N., Searle, A., Croft, M., Brewer, C., and Cole, M. (2007). Phenotype of autosomal dominant cone-rod dystrophy due to the R838C mutation of the GUCY2D gene encoding retinal guanylate cyclase-1. *Eye* *21*, 1220–1225. <https://doi.org/10.1038/sj.eye.6702612>.
- Kelsell, R.E., Gregory-Evans, K., Payne, A.M., Perrault, I., Kaplan, J., Yang, R.B., Garbers, D.L., Bird, A.C., Moore, A.T., and Hunt, D.M. (1998). Mutations in the retinal guanylate cyclase (RETGC-1) gene in dominant cone-rod dystrophy. *Hum. Mol. Genet.* *7*, 1179–1184. <https://doi.org/10.1093/hmg/7.7.1179>.
- Payne, A.M., Morris, A.G., Downes, S.M., Johnson, S., Bird, A.C., Moore, A.T., Bhattacharya, S.S., and Hunt, D.M. (2001). Clustering and frequency of mutations in the retinal guanylate cyclase (GUCY2D) gene in patients with dominant cone-rod dystrophies. *J. Med. Genet.* *38*, 611–614.
- Wilkie, S.E., Newbold, R.J., Deery, E., Walker, C.E., Stinton, I., Ramamurthy, V., Hurley, J.B., Bhattacharya, S.S., Warren, M.J., and Hunt, D.M. (2000). Functional characterization of missense mutations at codon 838 in retinal guanylate cyclase correlates with disease severity in patients with autosomal dominant cone-rod dystrophy. *Hum. Mol. Genet.* *9*, 3065–3073.
- Dizhoor, A.M., Lowe, D.G., Olshevskaya, E.V., Laura, R.P., and Hurley, J.B. (1994). The human photoreceptor membrane guanylyl cyclase, RetGC, is present in outer segments and is regulated by calcium and a soluble activator. *Neuron* *12*, 1345–1352. [https://doi.org/10.1016/0896-6273\(94\)90449-9](https://doi.org/10.1016/0896-6273(94)90449-9).
- Nikonov, S.S., Filatov, G.N., and Fesenko, E.E. (1993). On the activation of phosphodiesterase by a 26 kDa protein. *FEBS Lett.* *316*, 34–36. [https://doi.org/10.1016/0014-5793\(93\)81731-e](https://doi.org/10.1016/0014-5793(93)81731-e).
- Yee, R., and Liebman, P.A. (1978). Light-activated phosphodiesterase of the rod outer segment. Kinetics and parameters of activation and deactivation. *J. Biol. Chem.* *253*, 8902–8909.
- Fesenko, E.E., Kolesnikov, S.S., and Lyubarsky, A.L. (1985). Induction by cyclic GMP of cationic conductance in plasma membrane of retinal rod outer segment. *Nature* *313*, 310–313. <https://doi.org/10.1038/313310a0>.
- Peshenko, I.V., and Dizhoor, A.M. (2006). Ca²⁺ and Mg²⁺ binding properties of GCAP-1. Evidence that Mg²⁺-bound form is the physiological activator of photoreceptor guanylyl cyclase. *J. Biol. Chem.* *281*, 23830–23841. <https://doi.org/10.1074/jbc.M600257200>.
- Peshenko, I.V., Olshevskaya, E.V., and Dizhoor, A.M. (2015). Evaluating the role of retinal membrane guanylyl cyclase 1 (RetGC1) domains in binding guanylyl cyclase-activating proteins (GCAPs). *J. Biol. Chem.* *290*, 6913–6924. <https://doi.org/10.1074/jbc.M114.629642>.
- Peshenko, I.V., Moiseyev, G.P., Olshevskaya, E.V., and Dizhoor, A.M. (2004). Factors that determine Ca²⁺ sensitivity of photoreceptor guanylyl cyclase. Kinetic analysis of the interaction between the Ca²⁺-bound and the Ca²⁺-free guanylyl cyclase activating proteins (GCAPs) and recombinant photoreceptor guanylyl cyclase 1 (RetGC-1). *Biochemistry* *43*, 13796–13804. <https://doi.org/10.1021/bi048943m>.
- Peshenko, I.V., Olshevskaya, E.V., Azadi, S., Molday, L.L., Molday, R.S., and Dizhoor, A.M. (2011). Retinal degeneration 3 (RD3) protein inhibits catalytic activity of retinal membrane guanylyl cyclase (RetGC) and its stimulation by activating proteins. *Biochemistry* *50*, 9511–9519. <https://doi.org/10.1021/bi201342b>.
- Peshenko, I.V., Olshevskaya, E.V., and Dizhoor, A.M. (2016). Functional study and mapping sites for interaction with the target enzyme in retinal degeneration 3 (RD3) protein. *J. Biol. Chem.* *291*, 19713–19723. <https://doi.org/10.1074/jbc.M116.742288>.
- Sato, S., Peshenko, I.V., Olshevskaya, E.V., Kefalov, V.J., and Dizhoor, A.M. (2018). GUCY2D cone-rod dystrophy-6 is a "phototransduction disease" triggered by abnormal calcium feedback on retinal membrane guanylyl cyclase 1. *J. Neurosci.* *38*, 2990–3000. <https://doi.org/10.1523/JNEUROSCI.2985-17.2018>.
- Plana-Bonamaisó, A., López-Begines, S., Andilla, J., Fidalgo, M.J., Loza-Alvarez, P., Estanyol, J.M., Villa, P.d.l., and Méndez, A. (2020). GCAP neuronal calcium sensor proteins mediate photoreceptor cell death in the rd3 mouse model of LCA12 congenital blindness by involving endoplasmic reticulum stress. *Cell Death Dis.* *11*, 62. <https://doi.org/10.1038/s41419-020-2255-0>.
- Dizhoor, A.M., Olshevskaya, E.V., and Peshenko, I.V. (2019). Retinal guanylyl cyclase activation by calcium sensor proteins mediates photoreceptor degeneration in an rd3 mouse model of congenital human blindness. *J. Biol. Chem.* *294*, 13729–13739. <https://doi.org/10.1074/jbc.RA119.009948>.
- Peshenko, I.V., Olshevskaya, E.V., and Dizhoor, A.M. (2020). GUCY2D mutations in retinal guanylyl cyclase 1 provide biochemical reasons for dominant cone-rod dystrophy but not for stationary night blindness. *J. Biol. Chem.* *295*, 18301–18315. <https://doi.org/10.1074/jbc.RA120.015553>.
- McCullough, K.T., Boye, S.L., Fajardo, D., Calabro, K., Peterson, J.J., Strang, C.E., Chakraborty, D., Gloskowski, S., Haskett, S., Samuelsson, S., et al. (2019). Somatic gene editing of GUCY2D by AAV-CRISPR/Cas9 alters retinal structure and function in mouse and macaque. *Hum. Gene Ther.* *30*, 571–589. <https://doi.org/10.1089/hum.2018.193>.
- Dizhoor, A.M., Olshevskaya, E.V., and Peshenko, I.V. (2016). The R838S mutation in retinal guanylyl cyclase 1 (RetGC1) alters calcium sensitivity of cGMP synthesis in the retina and causes blindness in transgenic mice. *J. Biol. Chem.* *291*, 24504–24516. <https://doi.org/10.1074/jbc.M116.755553>.
- Giannoukos, G., Ciulla, D.M., Marco, E., Abdulkerim, H.S., Barrera, L.A., Bothmer, A., Dhanapal, V., Gloskowski, S.W., Jayaram, H., Maeder, M.L., et al. (2018). UDI^{TA}™, a genome editing detection method for indels and genome rearrangements. *BMC Genom.* *19*, 212. <https://doi.org/10.1186/s12864-018-4561-9>.
- Boye, S.L., Conlon, T., Erger, K., Ryals, R., Neeley, A., Cossette, T., Pang, J., Dyka, F.M., Hauswirth, W.W., and Boye, S.E. (2011). Long-term preservation of cone photoreceptors and restoration of cone function by gene therapy in the guanylate cyclase-1 knockout (GC1KO) mouse. *Invest. Ophthalmol. Vis. Sci.* *52*, 7098–7108. <https://doi.org/10.1167/iovs.11-7867>.
- Boye, S.L., Peterson, J.J., Choudhury, S., Min, S.H., Ruan, Q., McCullough, K.T., Zhang, Z., Olshevskaya, E.V., Peshenko, I.V., Hauswirth, W.W., et al. (2015). Gene Therapy Fully Restores Vision to the All-Cone Nrl(-/-) Gucy2e(-/-) Mouse Model of Leber Congenital Amaurosis-1. *Hum. Gene Ther.* *26*, 575–592. <https://doi.org/10.1089/hum.2015.053>.
- Wu, W.H., Tsai, Y.T., Huang, I.W., Cheng, C.H., Hsu, C.W., Cui, X., Ryu, J., Quinn, P.M.J., Caruso, S.M., Lin, C.S., and Tsang, S.H. (2022). CRISPR genome surgery in a novel humanized model for autosomal dominant retinitis pigmentosa. *Mol. Ther.* *30*, 1407–1420. <https://doi.org/10.1016/j.ymthe.2022.02.010>.
- Tsai, Y.T., Wu, W.H., Lee, T.T., Wu, W.P., Xu, C.L., Park, K.S., Cui, X., Justus, S., Lin, C.S., Jauregui, R., et al. (2018). Clustered regularly interspaced short palindromic repeats-based genome surgery for the treatment of autosomal dominant retinitis pigmentosa. *Ophthalmology* *125*, 1421–1430. <https://doi.org/10.1016/j.ophtha.2018.04.001>.
- Baehr, W., Karan, S., Maeda, T., Luo, D.G., Li, S., Bronson, J.D., Watt, C.B., Yau, K.W., Frederick, J.M., and Palczewski, K. (2007). The function of guanylate cyclase 1 and guanylate cyclase 2 in rod and cone photoreceptors. *J. Biol. Chem.* *282*, 8837–8847. <https://doi.org/10.1074/jbc.M610369200>.
- Boye, S.L., Peshenko, I.V., Huang, W.C., Min, S.H., McDoom, I., Kay, C.N., Liu, X., Dyka, F.M., Foster, T.C., Umino, Y., et al. (2013). AAV-mediated gene therapy in the guanylate cyclase (RetGC1/RetGC2) double knockout mouse model of Leber congenital amaurosis. *Hum. Gene Ther.* *24*, 189–202. <https://doi.org/10.1089/hum.2012.193>.
- Karan S, Frederick JM, Baehr W. Novel functions of photoreceptor guanylate cyclases revealed by targeted deletion. *Mol. Cell. Biochem.* *334*, 141–155. <https://doi.org/10.1007/s11010-009-0322-z>.
- Yang, R.B., Robinson, S.W., Xiong, W.H., Yau, K.W., Birch, D.G., and Garbers, D.L. (1999). Disruption of a retinal guanylyl cyclase gene leads to cone-specific dystrophy and paradoxical rod behavior. *J. Neurosci.* *19*, 5889–5897. <https://doi.org/10.1523/jneurosci.19-14-05889.1999>.

30. Coleman, J.E., Zhang, Y., Brown, G.A.J., and Semple-Rowland, S.L. (2004). Cone cell survival and downregulation of GCAP1 protein in the retinas of GC1 knockout mice. *Invest. Ophthalmol. Vis. Sci.* 45, 3397–3403. <https://doi.org/10.1167/iops.04-0392>.
31. Stanescu, B., and Michiels, J. (1976). Electroretinography and temporal aspects in macular dystrophy. *Ophthalmologica* 172, 367–378. <https://doi.org/10.1159/000307736>.
32. Rabb, M.F., Tso, M.O., and Fishman, G.A. (1986). Cone-rod dystrophy. A clinical and histopathologic report. *Ophthalmology* 93, 1443–1451. [https://doi.org/10.1016/s0161-6420\(86\)33547-4](https://doi.org/10.1016/s0161-6420(86)33547-4).
33. Ait-Ali, N., Fridlich, R., Millet-Puel, G., Clérin, E., Delalande, F., Jaillard, C., Blond, F., Perrocheau, L., Reichman, S., Byrne, L.C., et al. (2015). Rod-derived cone viability factor promotes cone survival by stimulating aerobic glycolysis. *Cell* 161, 817–832. <https://doi.org/10.1016/j.cell.2015.03.023>.
34. Bae, S., Park, J., and Kim, J.S. (2014). Cas-OFFinder: a fast and versatile algorithm that searches for potential off-target sites of Cas9 RNA-guided endonucleases. *Bioinformatics* 30, 1473–1475. <https://doi.org/10.1093/bioinformatics/btu048>.
35. Lowe, D.G., Dizhoor, A.M., Liu, K., Gu, Q., Spencer, M., Laura, R., Lu, L., and Hurley, J.B. (1995). Cloning and expression of a second photoreceptor-specific membrane retina guanylyl cyclase (RetGC), RetGC-2. *Proc. Natl. Acad. Sci. USA* 92, 5535–5539. <https://doi.org/10.1073/pnas.92.12.5535>.
36. Khani, S.C., Pawlyk, B.S., Bulgakov, O.V., Kasperek, E., Young, J.E., Adamian, M., Sun, X., Smith, A.J., Ali, R.R., and Li, T. (2007). AAV-mediated expression targeting of rod and cone photoreceptors with a human rhodopsin kinase promoter. *Invest. Ophthalmol. Vis. Sci.* 48, 3954–3961. <https://doi.org/10.1167/iops.07-0257>.
37. Zolotukhin, S., Potter, M., Zolotukhin, I., Sakai, Y., Loiler, S., Fraites, T.J., Jr., Chiodo, V.A., Phillipsberg, T., Muzyczka, N., Hauswirth, W.W., et al. (2002). Production and purification of serotype 1, 2, and 5 recombinant adeno-associated viral vectors. *Methods* 28, 158–167.
38. Timmers, A.M., Zhang, H., Squitieri, A., and Gonzalez-Pola, C. (2001). Subretinal injections in rodent eyes: effects on electrophysiology and histology of rat retina. *Mol. Vis.* 7, 131–137.
39. Weymouth, A.E., and Vingrys, A.J. (2008). Rodent electroretinography: methods for extraction and interpretation of rod and cone responses. *Prog. Retin. Eye Res.* 27, 1–44. <https://doi.org/10.1016/j.preteyeres.2007.09.003>.
40. Pang, J.J., Dai, X., Boye, S.E., Barone, I., Boye, S.L., Mao, S., Everhart, D., Dinculescu, A., Liu, L., Umino, Y., et al. (2011). Long-term retinal function and structure rescue using capsid mutant AAV8 vector in the rd10 mouse, a model of recessive retinitis pigmentosa. *Mol. Ther.* 19, 234–242. <https://doi.org/10.1038/mt.2010.273>.
41. Dietrich, M., Hecker, C., Hilla, A., Cruz-Herranz, A., Hartung, H.P., Fischer, D., Green, A., and Albrecht, P. (2019). Using optical coherence tomography and optokinetic response as structural and functional visual system readouts in mice and rats. *J. Vis. Exp.* 10, 143. <https://doi.org/10.3791/58571>.
42. Bosch, M. (2019). Introduction to ImageJ macro language in a particle counting analysis: automation matters. *Methods Mol. Biol.* 2040, 51–70. https://doi.org/10.1007/978-1-4939-9686-5_4.